**Nao-Aki Noda**
Department of Mechanical Engineering,
Kyushu Institute of Technology,
Kitakyushu 804-8550, Japan
e-mail: noda@kyutech.ac.jp

**Masato Nagawa**

**Fumitaka Shiraishi**

Daiso Corporation,
Kitakyushu 804-0061, Japan

**Akifumi Inoue**
Department of Mechanical Engineering,
Kyushu Institute of Technology,
Kitakyushu 804-8550, Japan

# Sealing Performance of New Gasketless Flange

*This paper deals with a new seal system between two flanges without using gaskets. The system includes a groove and an annular lip that is held by one of the flange with its highest point in contact with the other flange to form a seal line when the flanges are assembled. The condition whether the system leaks or not depends on the shape and dimension of the annular lip and its deformation during the contact. In this study, several gasketless flanges are prepared with different lip dimensions to investigate the contact and sealing condition through an experimental and FEM analyses. The analyses indicate that the conditions can be expressed in terms of the maximum contact stress and the plastic zone size when the flanges are assembled. The helium leak testing reveals that the gasketless flange has better sealing performance compared to conventional gaskets.*
[DOI: 10.1115/1.1464876]

*Keywords: Fixing Element, Coupling, Machine Element, Stress Analysis, Finite Element Method, Contact Problem, Pipe Flange, Sealing Performance*

## 1 Introduction

It is known that the toxic air pollution problem is widespread. In 1987 industry reports suggest that an estimated 2.7 billion lb of toxic air pollutants were emitted into the atmosphere, contributing to approximately 300–1500 cancer fatalities annually. The Clean Air Act of 1990 [1] offers a comprehensive plan for achieving significant reductions in emissions of hazardous air pollutants from major sources. The new law includes a list of 189 toxic air pollutants of which emissions must be reduced. From this viewpoint, it is desirable to develop a new seal system for pipe flanges in industrial plants that requires little or no maintenance.

In flange joints it is always necessary to select a suitable gasket depending on the kind of fluid, the pressure and the temperature being used. Table 1 indicates several types of gaskets classified according to fluids, pressures and temperatures [2]. However, even though suitable gaskets are chosen, their sealing performance usually deteriorates over the years. Therefore, maintenance to repair leaks and/or replace gaskets is required. In this paper a new seal system between two flanges without using gaskets has been treated [3]. Figure 1(*a*) shows the system that includes a groove and an annular lip that is machined in one of the flange and being in contact with the other flange to form a seal line when the flanges are assembled. Figure 1(*b*) shows a kind of gasket using the equivalent seal system. This new gasket is named superseal [2], which is to be inserted between the flanges instead of conventional gaskets. In this study several gasketless flanges are machined with different dimensions of the annular lip to investigate the contact and sealing conditions through experimental and FEM analyses.

## 2 Experimental Method for Water Leak Testing and Results

Table 2 and Fig. 2 give the detailed shape and dimensions of models used for water leak testing and FEM analysis. By comparing the results of models A and B, we may find how sealing is achieved by self-energized action on the annular lip. From the results of models B and C, we may find a suitable dimension of the thickness $h$. From the results of models C and D, we may find a suitable dimension of the groove depth. The material used is 0.25 percent carbon steel, JIS S25C. The maximum surface roughness at the annular lip is $R_{max}=4\,\mu$m (JIS) and the maximum surface roughness of the other flange is $R_{max}=80\,\mu$m. Figure 3 shows the experimental equipment for water leak testing. After the flanges are clamped using M16 (JIS) bolts, an internal pressure of 4.9 MPa is applied to the flange models by means of a water-hydraulic pump. The results of water leak testing are shown in the right column of Table 2. Symbol ○ refers to no leakage for model B. Symbol △ refers to no leakage in the first trial but to the presence of leakage in the second trial, which is made once model A is assembled after deassembly. Symbol ● refers to leakage in the first trial in the case of model C. These experiments indicate that the sealing performance depends on the shape and dimension of the thin annular lip size, which is deformed during the contact. Currently, the authors think model B has the best dimensions because there has been no leakage, even after assembly and deassembly several times.

## 3 Numerical Finite Element Analysis and Results

Figure 4(*a*) indicates typical finite element mesh that uses 4-node axisymmetric element. Figure 4(*b*) shows material property used in the analysis. The total number of elements is between 2624~2961 and the total number of nodes is 2816~3173. The clamping force is about 98 kN and estimated from the torque applied to the bolts. This force is applied to the model through an equivalent axisymmetric uniform distributed load. The stress-strain curve used is indicated in Fig. 4, where Young's moduls $E$ is 206 GPa, Poisson's ratio $\nu$ is 0.3, and the yield stress is 255 MPa.

Figure 5 shows von Mises equivalent stresses for the gasketless flange and the superseal. As shown in Figs. 5(*a*) and (*b*), the states of stress are not very different. Therefore the results of FEM for superseals can be regarded as the ones of gasketless flanges. Figure 6 indicates the relationship between the clamping force and the contact length. For models B and C, if the clamping force is large enough, the contact length becomes almost a constant independent of the magnitude of the force.

Figure 7 shows von Mises equivalent stress. The maximum stresses $\sigma_{eq\,max}$ are almost equal for models A, B, C; that is, $\sigma_{eq\,max}=286$ MPa. On the other hand, the maximum normal stresses in the $z$ direction $\sigma_{z\,max}=-1200$ MPa for models A and

Contributed by the Pressure Vessels and Piping Division for publication in the JOURNAL OF PRESSURE VESSEL TECHNOLOGY. Manuscript received by the PVP Division, August 16, 2000; revised manuscript received November 2, 2001. Associate Editor: G. Hulbert.

  

Table 1 Several types of conventional gaskets

| Fluid | Type (use range of pressure and temperature) |
|---|---|
| • Steam<br>• Hot water | • Ring joint gasket(5~15MPa,773~873K)<br>• Corrugated metal gasket(2~10MPa,623~823K)<br>• Spiral wound gasket(2~10MPa,623~823K)<br>• Serrated metal gasket(2~10MPa,623~823K)<br>• Solid-metal flat gasket(2~10MPa,623~823K)<br>• Compressed asbestos sheet(0.5~4MPa,373~673K)<br>• Compressed asbestos sheet(2~5MPa,473~773K)<br>• Compressed asbestos sheet gasket reinforced with wire-netting(2~5MPa,473~773K)<br>• Rubber coated asbestos-cloth sheet gasket (2~5MPa,473~773K)<br>• Rubber coated asbestos-cloth sheet gasket reinforced with wire-netting(2~5MPa,473~773K)<br>• Rubber sheet gasket(0~2MPa,~373K)<br>• Cloth-inserted rubber sheet gasket (0~2MPa,~373K)<br>• Rubber seat gasket with wire-netting (0~2MPa,~373K) |
| • Fresh water<br>• Salt water<br>• Calcium chloride | • Compressed asbestos sheet(0~5MPa,563K)<br>• Rubber coated asbestos-cloth sheet gasket reinforced with wire-netting(0~5MPa,563K)<br>• Rubber sheet gasket(0~5MPa,373K)<br>• Cloth-inserted rubber sheet gasket (0~5MPa,373K)<br>• Rubber seat gasket with wire-netting (0~5MPa,373K) |
| • Air | • Rubber sheet gasket(0~2MPa,373K)<br>• Cloth-inserted rubber sheet gasket (0~2MPa,373K)<br>• Rubber seat gasket with wire-netting (0~2MPa,373K) |
| • Ammonia | • Spiral wound gasket(10MPa,773K)<br>• Compressed asbestos sheet(5MPa,773K)<br>• Teflon gasket(2MPa,203~533K) |

B, but $\sigma_{z\,max}=-900$ MPa for model C, which is smaller by about 25%. It may be concluded that the leakage of model C is caused by the small value of $\sigma_{z\,max}$. Stresses in the $z$ direction $\sigma_{z\,max}$ are shown to be about twice higher than the ultimate stress of Fig. 4(*b*) because triaxial state of stress appears at the contact region and therefore von Mises equivalent stresses $\sigma_{eq\,max}$ are not very high. The FEM results also indicate that for model A the plastic zone size around the contact region is larger. Because of this large plastic zone size, model A leaks after dismantling although there is no leakage in the first trial.

Finally, a suitable groove depth is considered because models A, B, C have a constant groove depth, $l=13$ mm. Fig. 7(*d*) shows the results for model D, where $l=8$ mm and $h=3$ mm. By reducing the depth the maximum stresses in the $z$ direction $\sigma_{z\,max}=-1300$ MPa with a suitable plastic zone size. However, around the root of the groove, the plastic zone prevails all over the section, and, therefore, the sealing performance seems deteriorated after dismantling.

The FEM analysis indicates that the conditions whether the system leaks or not can be controlled by the maximum contact stress $\sigma_{z\,max}$ and the plastic zone size when the flanges are assembled. The dimensions of model B provides a higher contact stress and a suitable plastic zone size. Suitable plastic deformations are necessary for good sealing because they rectify surface roughness at the contact area.

## 4 Method for Helium Leak Testing and Results

On the basis of the previous studies on the fundamental dimensions of the groove, helium leak testing based on JIS Z 2331-1992 (reaffirmed 1998) [4,5] is applied to the gasketless flange of model B and other flanges having conventional gaskets. Figure 8 shows the experimental equipment and Table 3 along with Fig. 2 indicate dimensions of models used for these tests. The test specimen nos. 1–6 are based on JIS flange B 2220 [6], and the test specimen nos. 7–8 are based on JPI flange 7S-15-93 [7]. The material used is 0.25 percent carbon steel, JIS S25C. For gasketless flanges nos. 9–11, the maximum surface roughness of the annular lip contact surface is $R_{max}=4$ $\mu$m (JIS) and the maximum surface roughness of the opposite flange making surface is $R_{max}=7$ $\mu$m. Several types of gaskets were prepared and tested under the specified pressure (see Table 4). Then, helium leak rates are

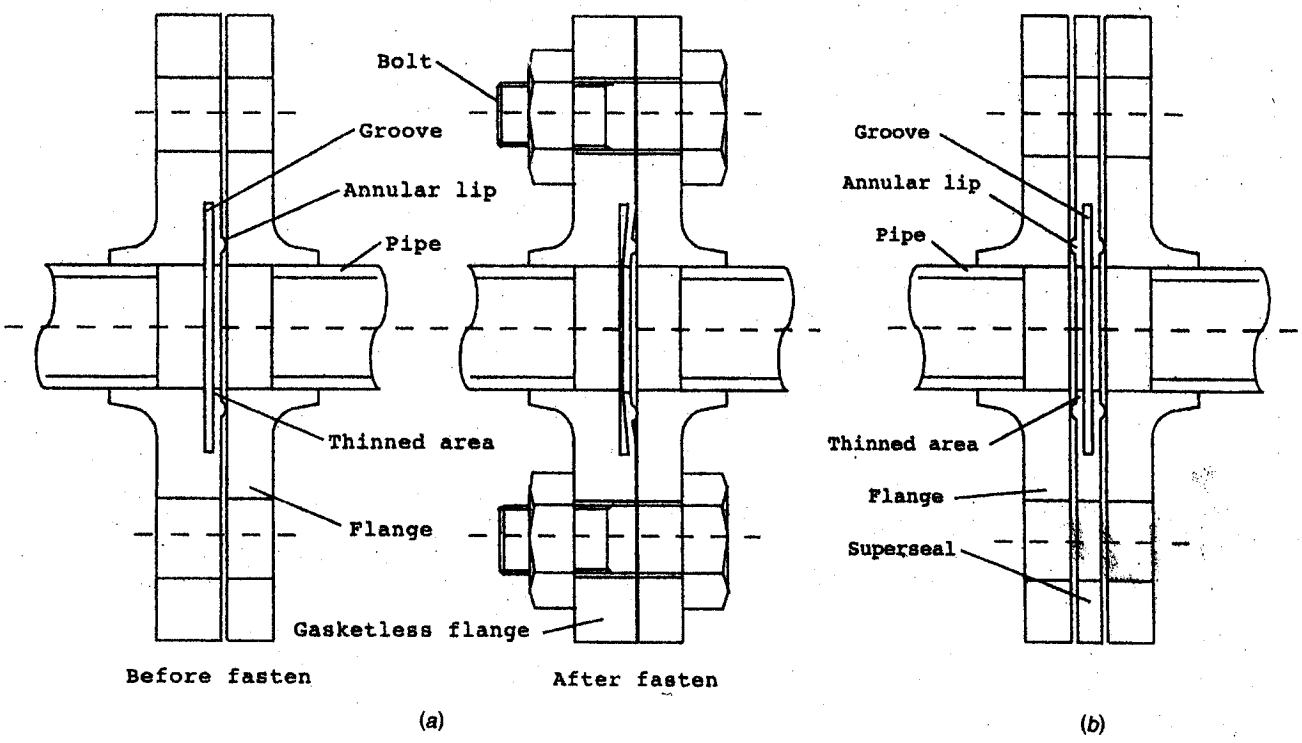


**Fig. 1** (*a*) Gasketless flange, and (*b*) a kind of gasket named superseal

**Table 2** Dimension of GL flange models for water leak testing (mm)

| | Model | a | b | c | d | e | f | g | h | i | Rj | Rk | l | experimental result |
|---|---|---|---|---|---|---|---|---|---|---|---|---|---|---|
| no groove | A | 155 | 120 | — | 67.0 | 61.0 | 24.0 | 0 | ∞ | 0.2 | 1.5 | 4.0 | — | △ Water 4.9MPa |
| h=5mm | B | 155 | 120 | 87.0 | 67.0 | 61.0 | 24.0 | 3.0 | 5.0 | 0.2 | 1.5 | 4.0 | 13.0 | ○ Water 4.9MPa |
| h=3mm | C | 155 | 120 | 87.0 | 67.0 | 61.0 | 24.0 | 3.0 | 3.0 | 0.2 | 1.5 | 4.0 | 13.0 | ● Water 4.9MPa |
| l=8mm | D | 155 | 120 | 77.0 | 67.0 | 61.0 | 24.0 | 3.0 | 3.0 | 0.2 | 1.5 | 4.0 | 8.0 | — |

○:nonleak △:First nonleak, next leak ●:leak

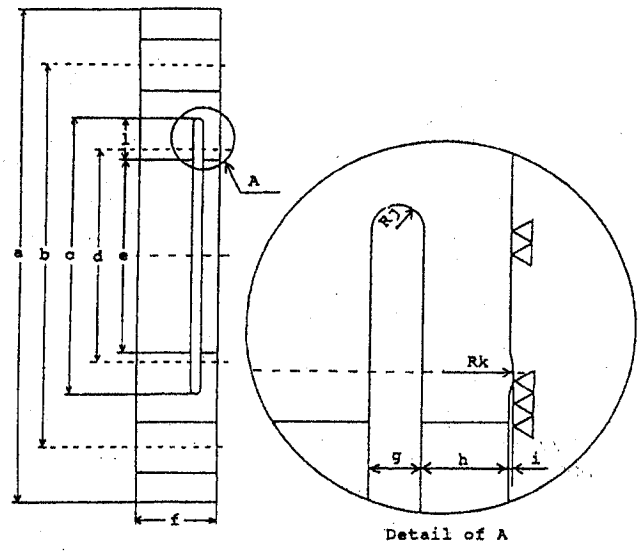


**Fig. 2** Dimension of GL flange models

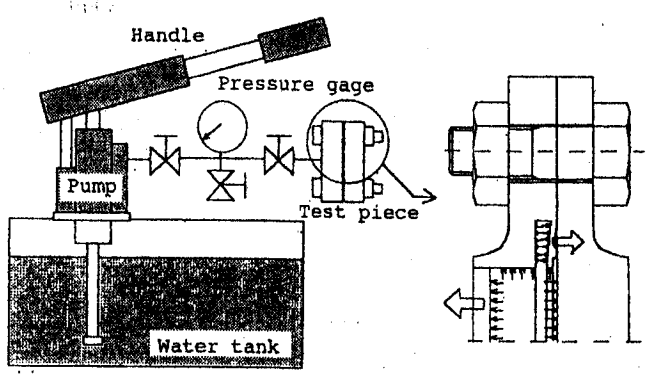


**Fig. 3** Experimental equipment for water leak testing

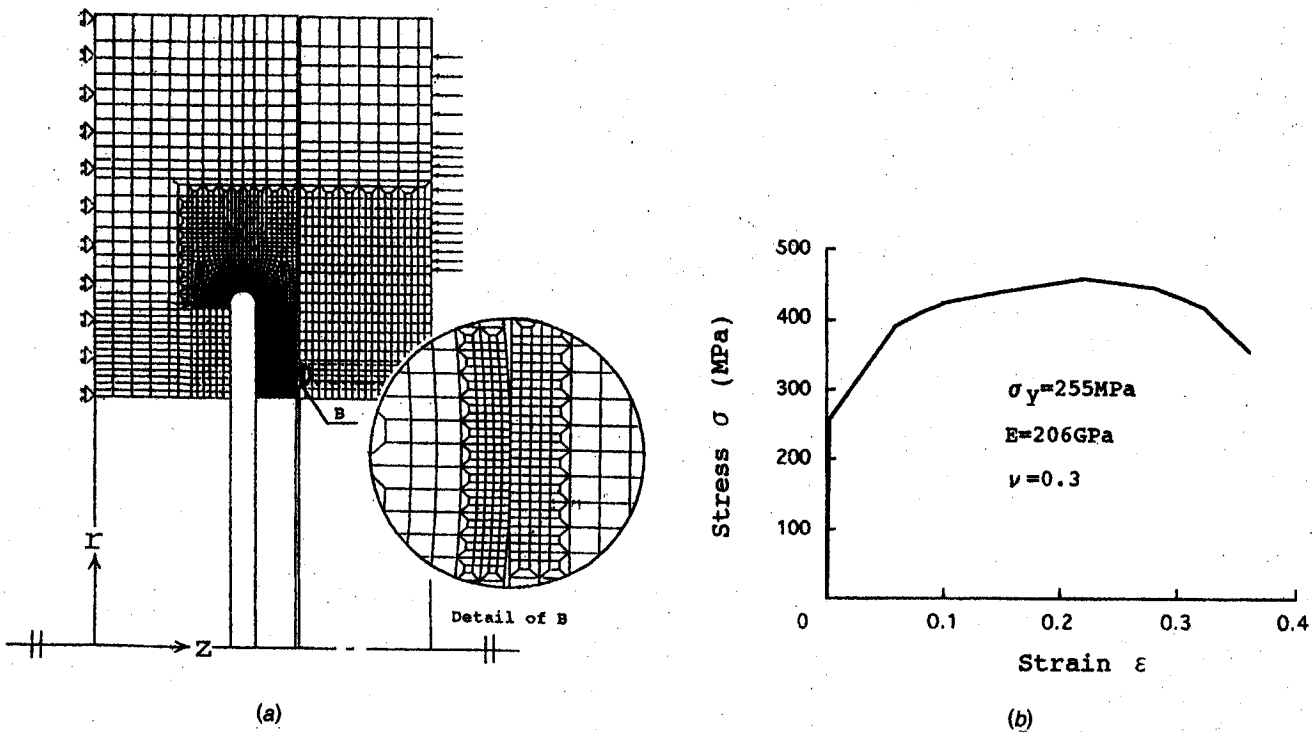


**Fig. 4 (*a*) Finite element mesh, and (*b*) material property**

measured. According to JIS Z 2331 [5], test pieces come up to the standard if leak rate is less than or equal to $1\times10^{-5}$ Pa·m$^3$/s. Figure 9 is a plot of the leak rate shown in Table 4. The average leak rate of conventional gaskets is about the standard leak rate, $1\times10^{-5}$ Pa·m$^3$/s. On the other hand, the gasketless flange has better sealing performance compared to the conventional gaskets.

Currently, the gasketless flanges of model B have been used in several plants for a few years with careful watch. Then, it is found that this configuration allows pressure and temperature fluctuations as those produced during start-up and shutdowns. The feasibility of the proposed design is also confirmed under cyclic loading because fatigue and leakage have not been seen.

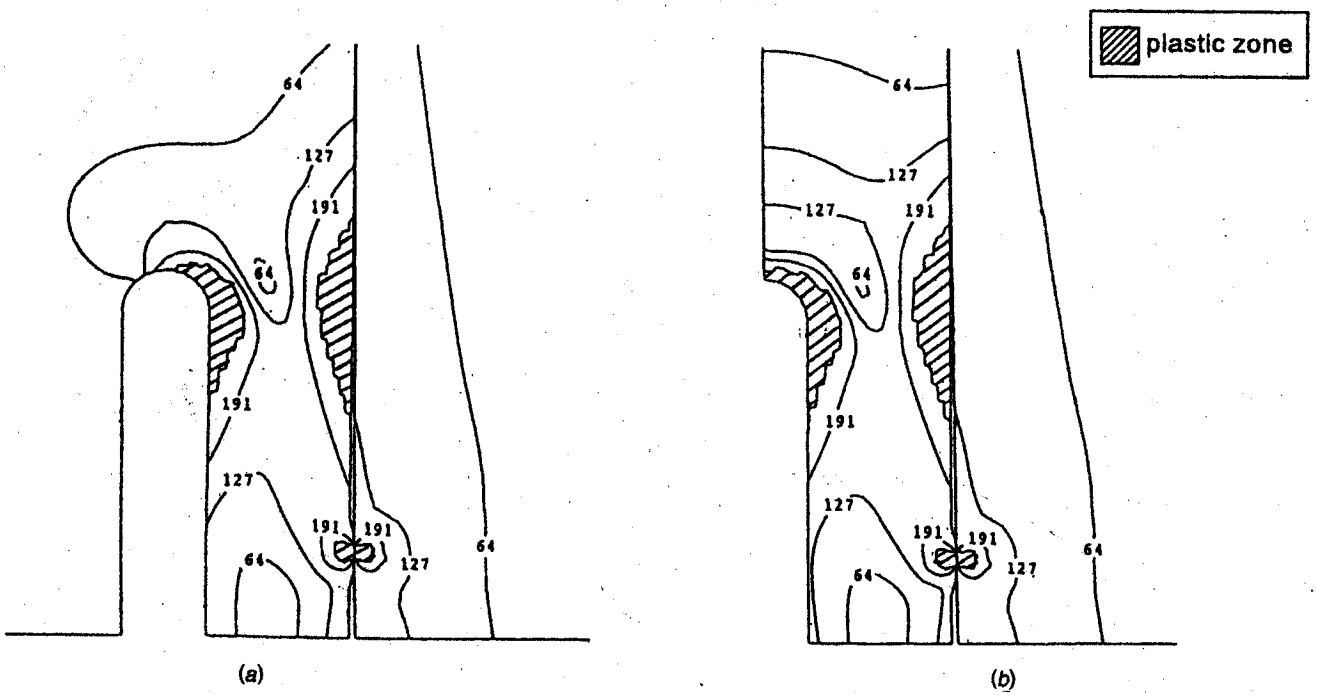


**Fig. 5 Mises equivalent stress $\sigma_{eq}$ (MPa) for (*a*) gasketless flange, and (*b*) a kind of gasket named superseal**

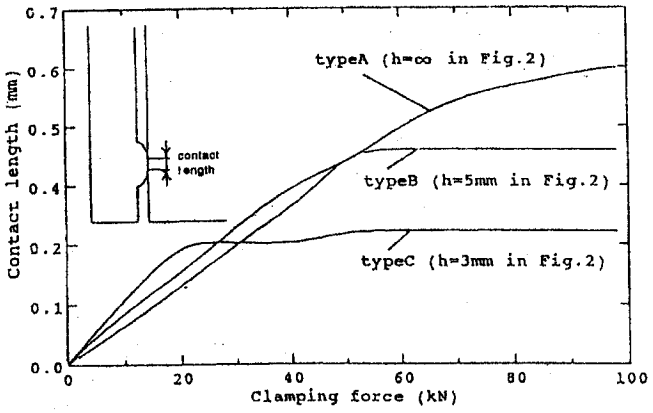


**Fig. 6 Contact length versus clamping force**

## 5 Conclusion

Generally, the sealing performance of gaskets of flange joints deteriorates after few years in service, and may result in leakage and eventually replace the gaskets. In this paper, a new seal is considered. In order to investigate the sealing mechanism, several gasketless flanges with different lip geometry have been considered. According to the experimental and FEM analyses, the following conclusions can be made:

1 Three experimental models A, B, C have been investigated. For model A, which has no groove, there is no leakage in the first trial. However, there appears leakage in the second trial after released and clamped again. There has been no leakage for model B, whose lip thickness is $h=5$ mm. There is leakage from the first-trial for model C, where $h=3$ mm. Through the experiment, it is found that the sealing performance depends on the shape and dimension of the lip, which deforms to form a seal line.

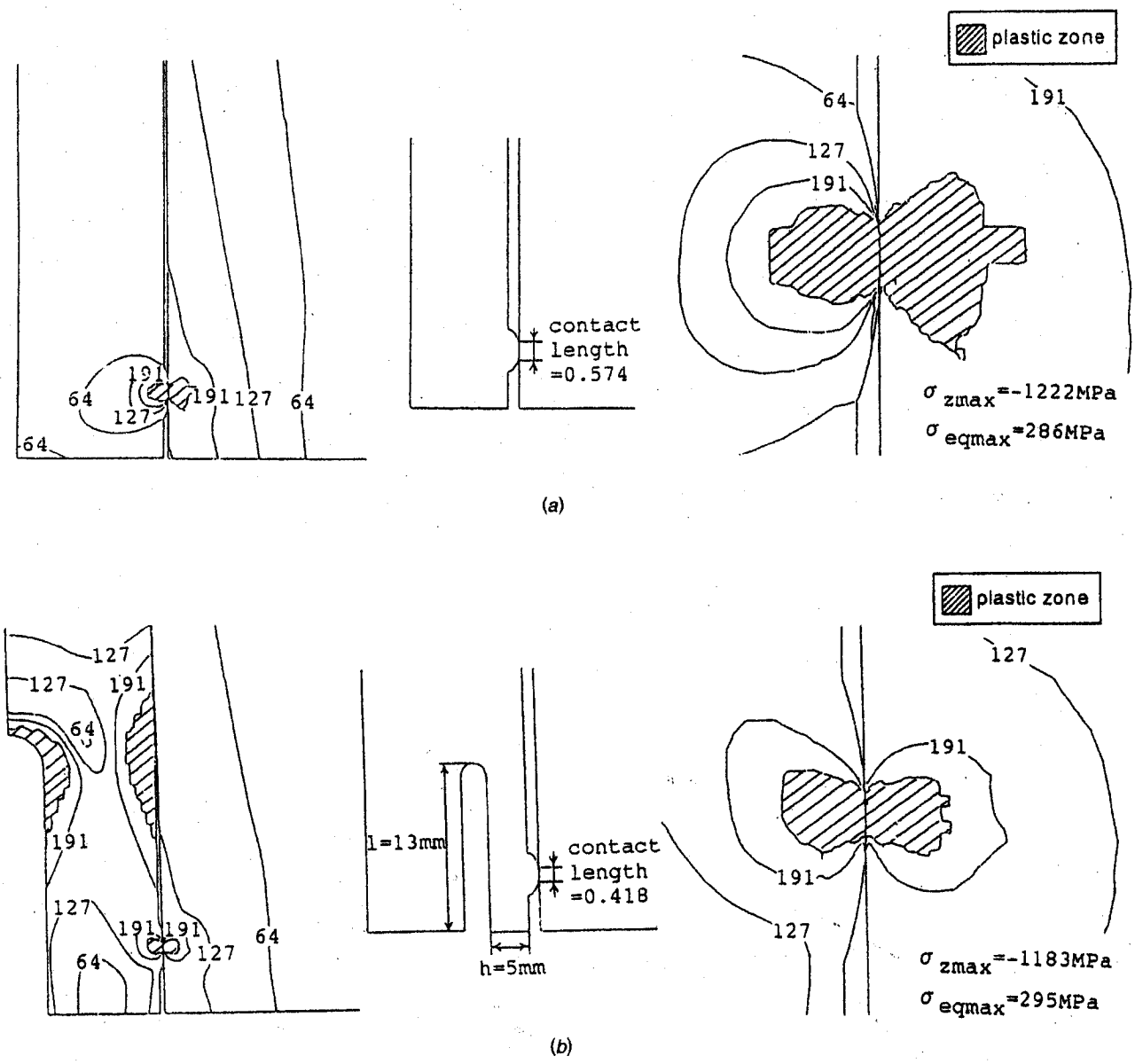


**Fig. 7 Equivalent stress $\sigma_{eq}$ (MPa)—(*a*) model A (no groove, $h=\infty$ in Fig. 2), (*b*) model B ($h=5$ mm in Fig. 2), (*c*) model C ($h=3$ mm in Fig. 2), (*d*) model D (1=8 mm in Fig. 2)**

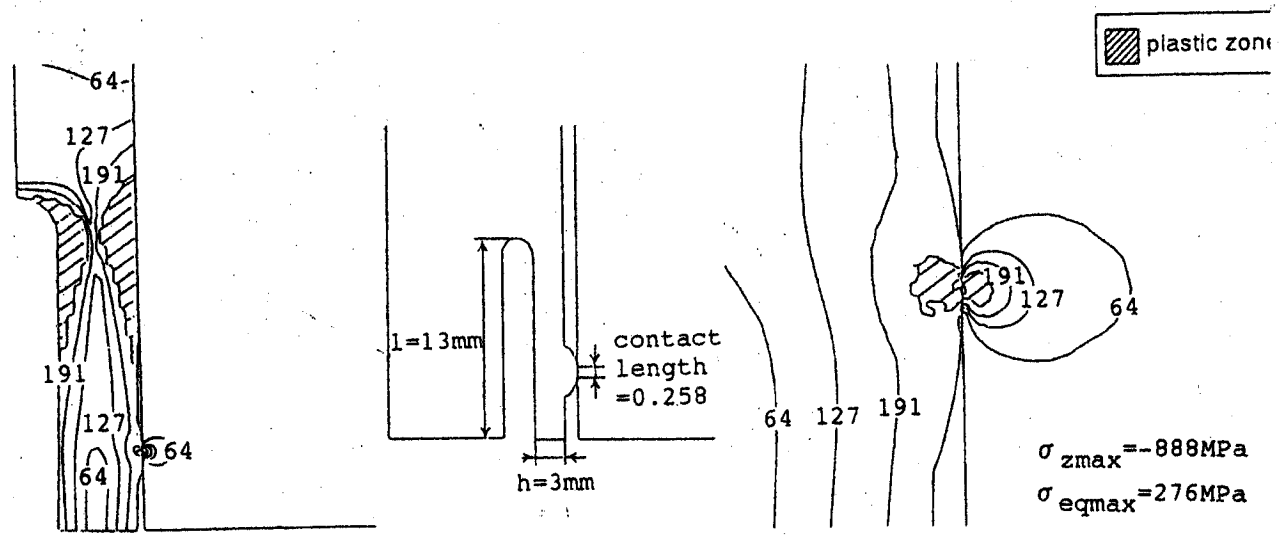


(c)

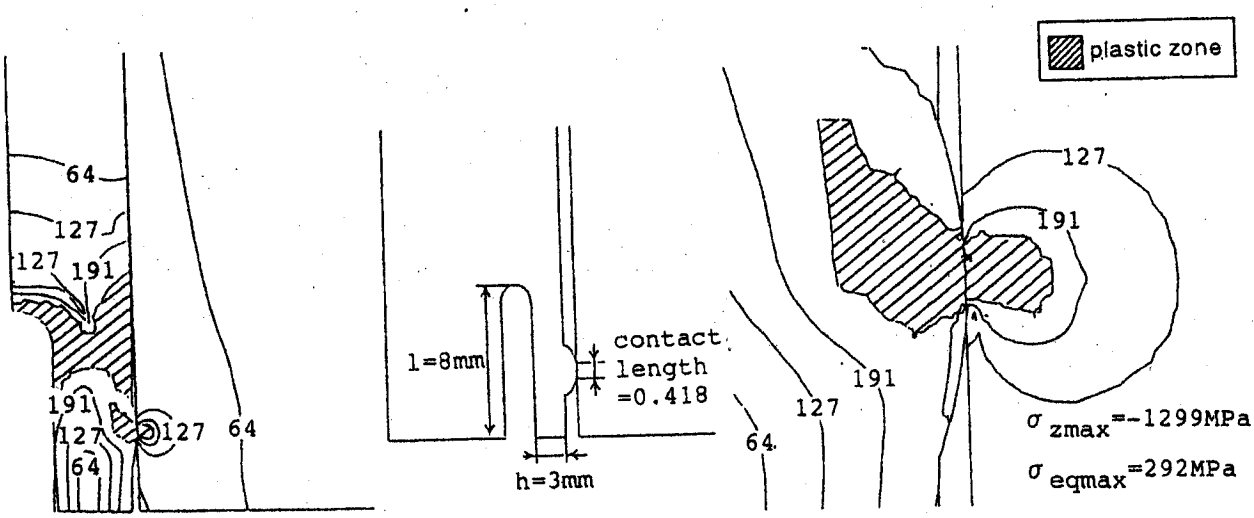


(d)

**Fig. 7 (continued)**

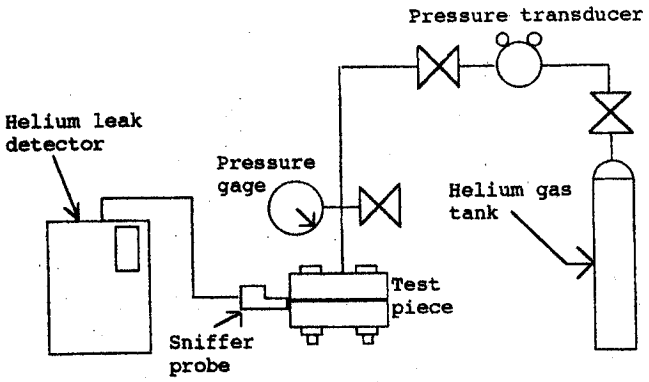


**Fig. 8 Experimental equipment for helium leak testing**

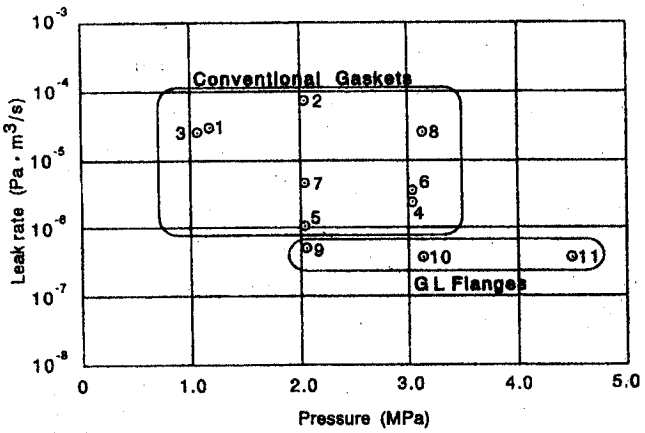


**Fig. 9 Helium leak rate versus internal pressure**

**Table 3 Dimension of conventional gasket flanges (nos. 1–8) and GL flanges (No. 9–11) for helium leak testing (mm)**

| Flange No. | a | b | c | d | e | f | g | h | i | Rj | Rk | l |
|---|---|---|---|---|---|---|---|---|---|---|---|---|
| 1 | 155 | 120 | - | - | 61.1 | 18 | - | - | 0 | - | - | - |
| 2 | 155 | 120 | - | - | 61.1 | 18 | - | - | 0 | - | - | - |
| 3 | 155 | 120 | - | - | 61.1 | 18 | - | - | 0 | - | - | - |
| 4 | 165 | 130 | - | - | 61.1 | 22 | - | - | 0 | - | - | - |
| 5 | 155 | 120 | - | - | 61.1 | 21 | - | - | 0 | - | - | - |
| 6 | 165 | 130 | - | - | 61.1 | 25 | - | - | 0 | - | - | - |
| 7 | 152 | 120.6 | - | - | 61.1 | 31.35 | - | - | 0 | - | - | - |
| 8 | 152 | 120.6 | - | - | 61.1 | 31.35 | - | - | 0 | - | - | - |
| 9 (B) | 155 | 120 | 87.1 | 67.1 | 61.1 | 24.0 | 3.0 | 5.0 | 0.2 | 1.5 | 4.0 | 13.0 |
| 10 (B*) | 155 | 120 | 88.5 | 70.0 | 61.1 | 26.0 | 3.0 | 5.0 | 0.2 | 1.5 | 3.5 | 13.7 |
| 11 (B**) | 165 | 130 | 88.5 | 70.0 | 61.1 | 30.0 | 3.0 | 5.0 | 0.2 | 1.5 | 3.5 | 13.7 |

**Table 4 Dimension of convention gasket flanges (nos. 1–8) and L flanges (nos. 9–11) for helium leak testing (mm)**

| No. | Flange standards | Flange nominal pressure MPa{kgf/cm$^2$} | Flange nominal size | Types of gaskets | Test pressure Mpa | Leak rate Pa · m$^3$/s |
|---|---|---|---|---|---|---|
| 1 | JIS10K | 1.96{20} | 50A | Compressed asbestos sheet | 1.17 | $2.9\times10^{-5}$ |
| 2 | JIS20K | 4.90{50} | 50A | Compressed asbestos sheet | 2.05 | $7.4\times10^{-5}$ |
| 3 | JIS10K | 1.96{20} | 50A | Spiral wound gasket | 1.07 | $2.6\times10^{-5}$ |
| 4 | JIS30K | 7.95{75} | 50A | Spiral wound gasket | 3.04 | $2.4\times10^{-6}$ |
| 5 | JIS20K | 4.90{50} | 50A | O-ring V70 | 2.05 | $1.1\times10^{-6}$ |
| 6 | JIS30K | 7.95{75} | 50A | O-ring V70 | 3.04 | $3.6\times10^{-6}$ |
| 7 | JPI 150 | 1.03{11} =150 psi | 50A | Octagonal R22 | 2.05 | $4.7\times10^{-6}$ |
| 8 | JPI 150 | 1.03{11} =150 psi | 50A | Octagonal R22 | 3.13 | $2.6\times10^{-5}$ |
| 9 | GLF(B) | 1.96{20} | 50A | —— | 2.06 | $5.1\times10^{-7}$ |
| 10 | GLF(B*) | 4.90{50} | 50A | —— | 3.14 | $3.7\times10^{-7}$ |
| 11 | GLF(B**) | 7.95{75} | 50A | —— | 4.51 | $3.7\times10^{-7}$ |

2 FEM analysis indicates that the maximum stress at the contact zone, $\sigma_{z\,max} = -1200$ MPa with a suitable plastic zone size is necessary for good sealing performance. For example, model C leaks because of the small value of $\sigma_{z\,max} = -900$ MPa, and model A leaks in the second trial due to the larger plastic zone size at the contact region. It may be concluded that the dimensions of model B are desirable because of the large contact stress and suitable plastic zone size.

3 The helium leak testing indicates that the gasketless flange based on model B has less leak rate, and better sealing performance compared to conventional gaskets.

4 Currently, the gasketless flanges of model B have been used in several plants for a few years with careful watch. Then, it is found that this configuration allows pressure and temperature fluctuations as those produced during start-up and shutdowns. The feasibility of the proposed design is also confirmed under cyclic loading because fatigue and leakage have not been seen.

## Acknowledgment

The authors wish to express their thanks to Mr. Ken-Ichiro Takeuchi and Mr. Yasushi Takase for their FEM analysis and experimental work. The assistance and support given by the members of the research group, especially Dr. Hiroyuki Tanaka, Head of Fukuoka Interior Research Center, and Mr. Hiroshi Otsuji, President of Daiso Corporation, are greatly appreciated. This research has been partly supported by the joint research fund of Kitakyushu city and Fukuoka IST Foundation.

## References

[1] Home page, http://www.epa.gov/oar/oaq_caa.html
[2] Jun Akagawa, 1972, Seal Technology, 365-369, Kindaihenshusha (in Japanese).
[3] Nikkan-Kogyo Newspaper, Dec. 2. 1998, 37 (in Japanese).
[4] Hiroshi Otsuji, and Nagawa, Masato, Japan patent no. 2849345 (in Japanese); Hiroshi Otsuji and Masato Nagawa, USA patent (soon to appear).
[5] JIS Z 2331-1992 (Reaffirmed 1998), Method of Helium Leak Testing, Sniffer Method, pp. 17–20.
[6] JIS B 2220, 1995, JIS B 2238, 1996.
[7] 'PI STANDARD, Pipe Flange for the Petroleum Industry (Addenda-96), JPI-7S-15-93 (Addenda-96).